Wake fields and impedances simulations of LHC collimators with GdfidL code

Oscar Frasciello

INFN, Laboratori Nazionali di Frascati, Rome, Italy

4th Joint HiLumi LHC-LARP Annual Meeting, November, 2014
High Energy Accelerator Research Organization (KEK), Tsukuba, Japan, 17-21 November 2014

With contributions of: W. Bruns, S. Tomassini, M. Zobov, N. Biancacci, A. Grudiev, E. Metral, N. Mounet, B. Salvant, D. Alesini, A. Gallo

The HiLumi LHC Design Study is included in the High Luminosity LHC project and is partly funded by the European Commission within the Framework Programme 7 Capacities Specific Programme, Grant Agreement 284404

$\Re Z^{LHC}$

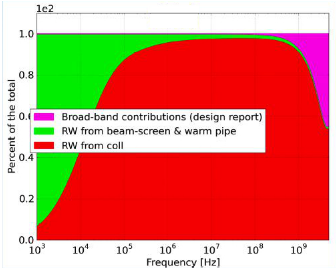

$\Im Z^{LHC}$

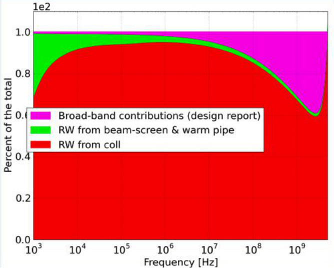

Collimator tune shifts

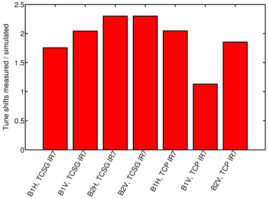

Total tune shifts

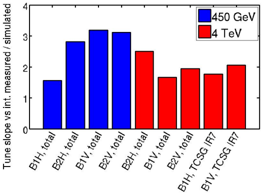

The need for LHC impedance model refining

- Resistive Wall (RW) impedance considered as the dominant contribution for LHC collimators impedance;
- In the "old" LHC model, geometric impedance was accounted for only in terms of round taper approximation;
- The existing LHC impedance model accounts only for a fraction, $\sim \frac{1}{3} - \frac{1}{2}$, of the measured transverse coherent tune shifts;

The factor of 2 arising from LHC tune shifts measurements vs. simualtions can be understood comparing the kick factors due to resistive wall impedance and the geometric impedance:

1. It's a quite straightforward way ;
2. Contributions from impedances having different frequency behaviour into the transverse tune shifts can be easily compared;
3. Only calculations of the broad band wakes are necessary without the exact knowledge of $Z(\omega)$;
4. Easily calculated by many numerical codes.

Geometric impedance: theoretical considerations II

Given $\xi = 0$ and $(m = 0)$ in Sacherer's formula for coherent mode frequency shift, one gets:

$$\Delta\omega_{c_0} = -\mathrm{C} \cdot I \sum_p \Im Z_T\,(\omega_p) e^{-\left(\frac{\omega\sigma_z}{c}\right)^2} \quad (1)$$

But from kick factor definition:

$$k_T = \frac{1}{2\pi} \int_{-\infty}^{\infty} \Im Z_T(\omega) |\lambda(\omega)|^2 \mathrm{d}\omega = \frac{1}{2\pi} \int_{-\infty}^{\infty} \Im Z_T(\omega) e^{-\left(\frac{\omega\sigma_z}{c}\right)^2} \mathrm{d}\omega \quad (2)$$

so that:

$$\boxed{\Delta\omega_0 \propto -k_T} \quad (3)$$

Real view

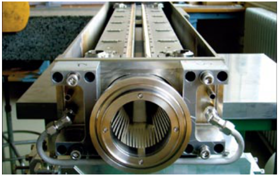

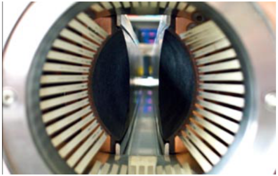

CAD design

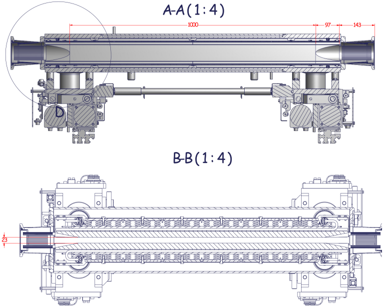

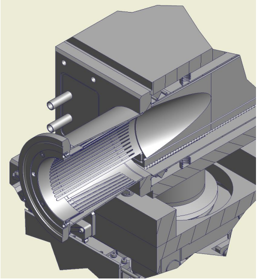

GdfidL electromagnetic code model

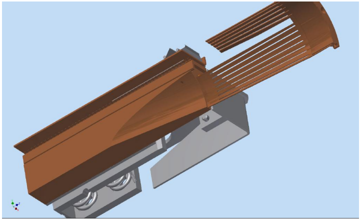

Very fine mesh needed for taper structure. We used 0.2 *mm* in all three directions, leading to several billions of mesh points ⇒ very huge computing task!

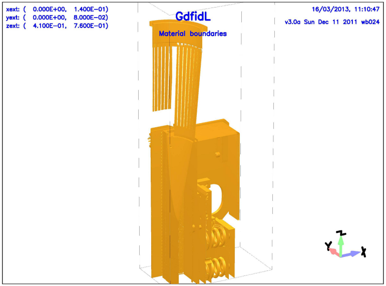

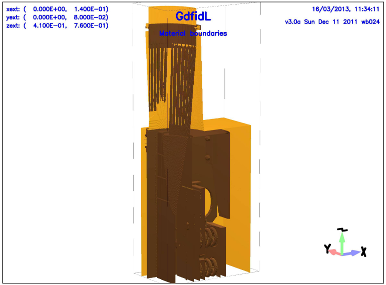

Geometric impedance: simulations II

Low frequency broad-band $Z_\perp$

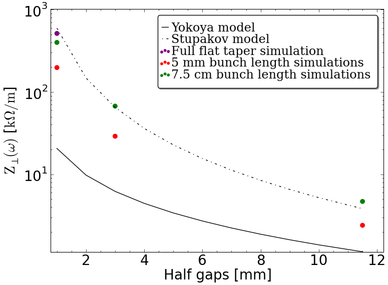

kick factor comparison

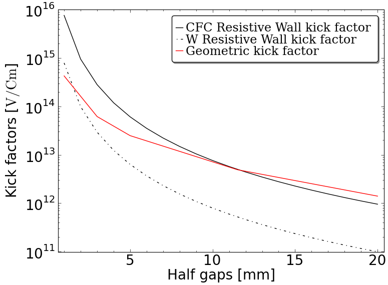

Models

1. $Z_T = j\frac{Z_0}{2\pi}\int\left(\frac{b'}{b}\right)^2 \mathrm{d}z;$
2. $Z_T = j\frac{Z_0 w}{4}\int\frac{(g')^2}{g^3}\mathrm{d}z;$

The Stupakov model in item 2 is closer to simulated points than that of Yokoya in item 1; there's only one point for the "full-flat" geometry below:

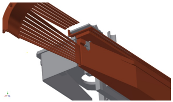

Geometric impedance: simulations II

1 *mm* half gap geometry

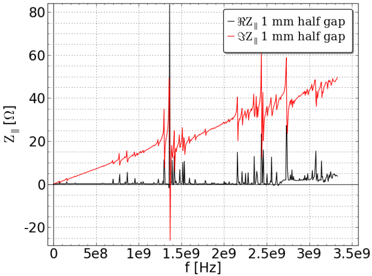

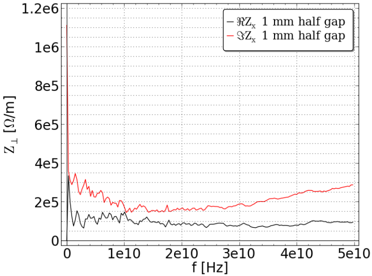

20 *mm* half gap geometry

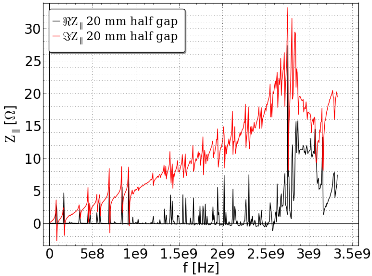

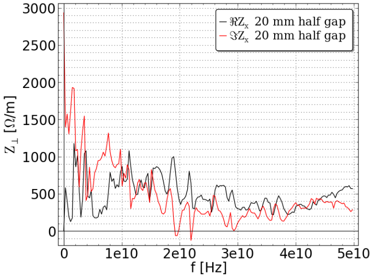

Geometric impedance: some comments on $Z_{\parallel}$

- Many resonant peaks at different frequencies are exhibited;
- These HOMs are created in the collimator tank, trapped between sliding contacts in the tapered transition area etc.[1];
- The parameters depend very much on the collimator gap size;
- Despite their shunt impedances are relatively small compared to typical HOMs in RF cavities, possible further RF losses and related collimator heating, due to these modes, in the conditions of higher circulating currents still need a deeper investigation.

[1] A. Grudiev, *Simulation of Longitudinal and Transverse Impedances of Trapped Modes in LHC Secondary Collimator*, **CERN AB-Note-2005-042**

A useful 3D view of what happens inside collimator

Wall currents on fingers and springs

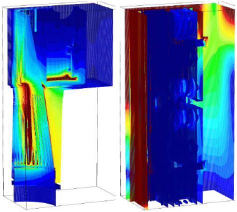

Inside the collimator...

...the H-field

Details of the various contributions in %

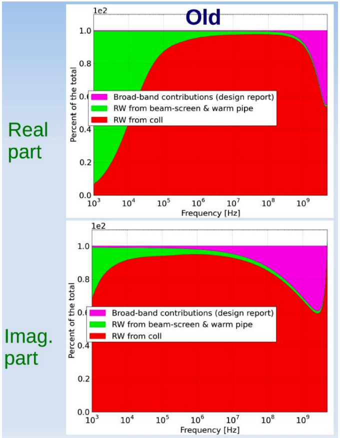

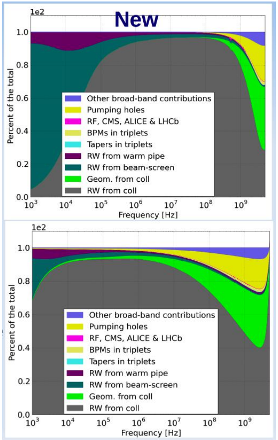

(Courtesy of N. Mounet)

The new BPM embedded collimator design

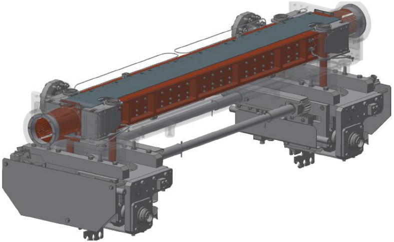

Preliminary estimation of new design contribution to impedance

	With BPM cavity	Without BPM cavity
Half gaps (*mm*)	$k_{\perp}(\frac{V}{Cm})$	$k_{\perp}(\frac{V}{Cm})$
1	$3.921 \cdot 10^{14}$	$3.340 \cdot 10^{14}$
3	$6.271 \cdot 10^{13}$	$5.322 \cdot 10^{13}$
5	$2.457 \cdot 10^{13}$	$2.124 \cdot 10^{13}$

The transverse effective impedance is expected to increase of about 20% wrt no BPM cavity collimator design.

The new BPM embedded collimator design

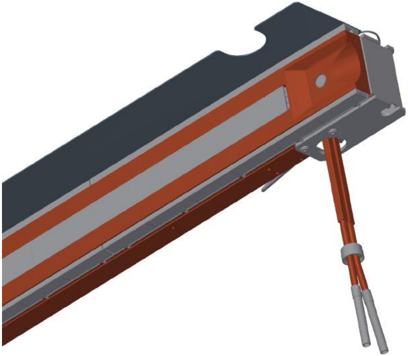

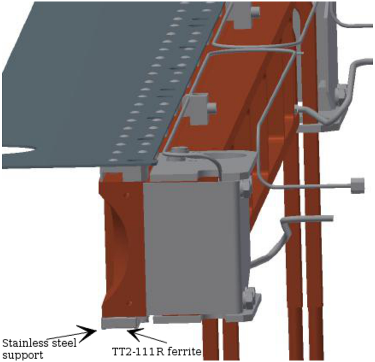

RF fingers are removed and their HOM damping functions are supposed to be supplied by TT2-111R ferrite blocks

New collimator design GdfidL model

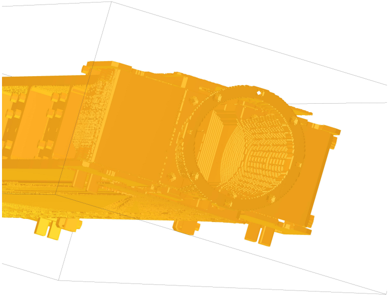

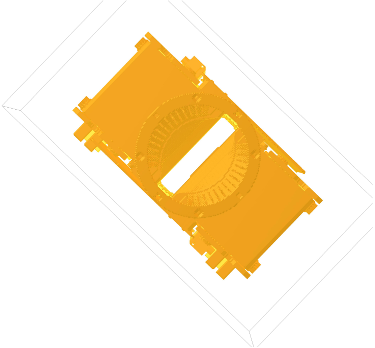

No more symmetry planes are applicable

$\Downarrow$

whole structure has to be simulated $\Rightarrow$ more simulation time needed

TT2-111R dispersive properties

μ experimental data (Courtesy of B. Salvant) & GdfidL DUT model

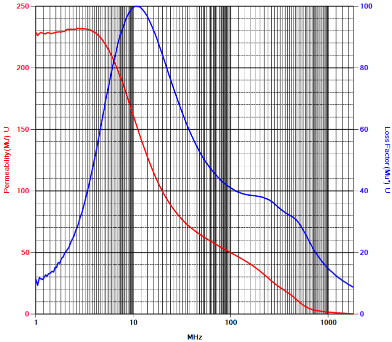

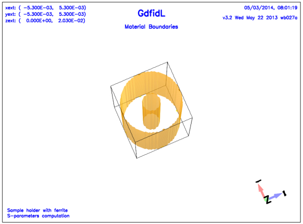

Data fits with n^th order Lorentz function & S_{11} results comparison

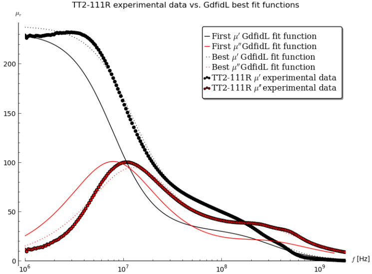

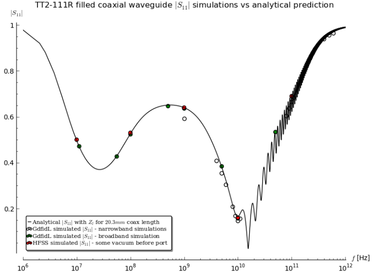

Benchmarking codes: CST, MMM, GdfidL

The simple pillbox geometry

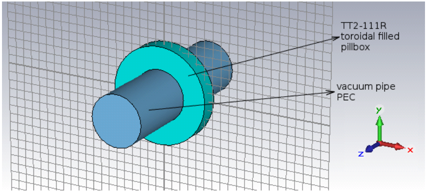

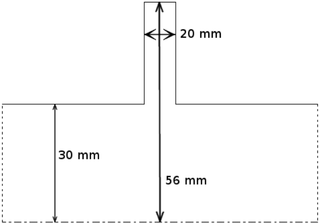

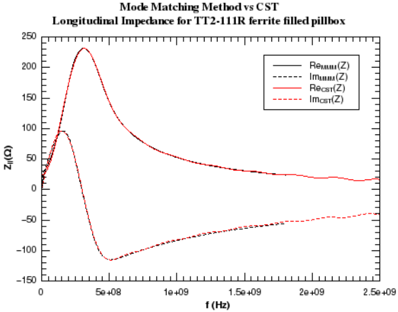

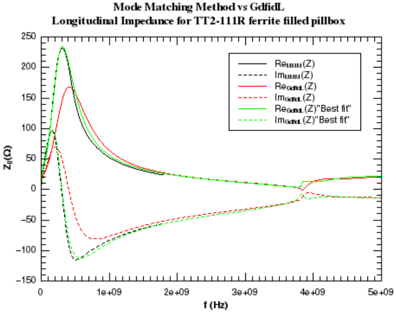

TT2-111R effects on new collimator design: $Z_{\|}$

Without TT2-111R

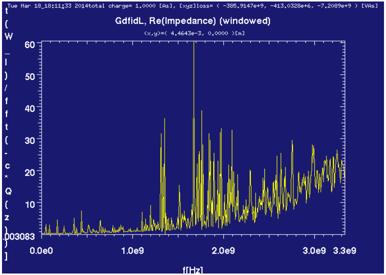

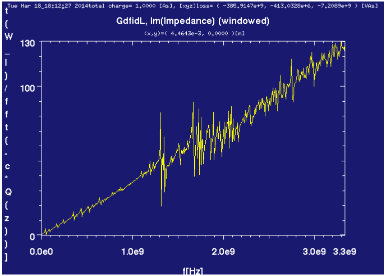

With TT2-111R

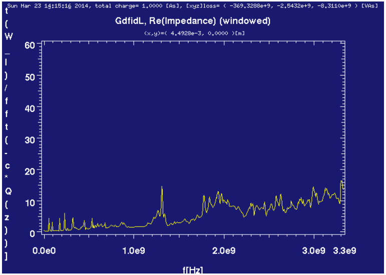

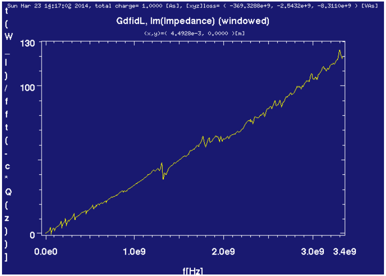

TT2-111R effects on new collimator design: $Z_\perp$

Without TT2-111R

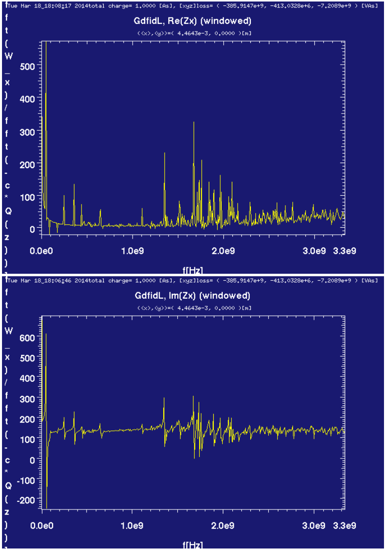

With TT2-111R

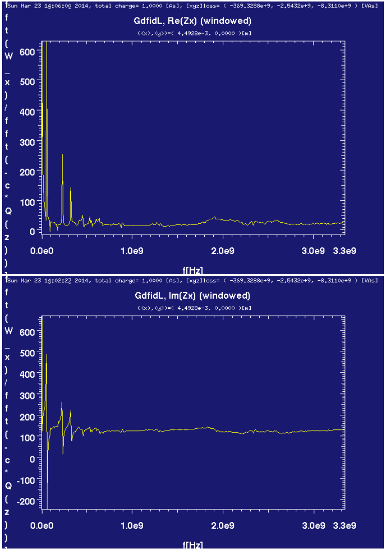

A bit more focus on low frequency

$\parallel$

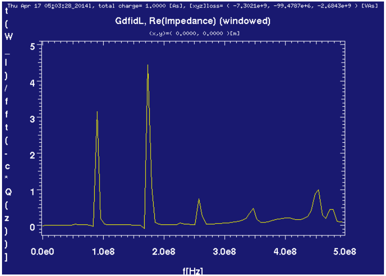

$\perp$

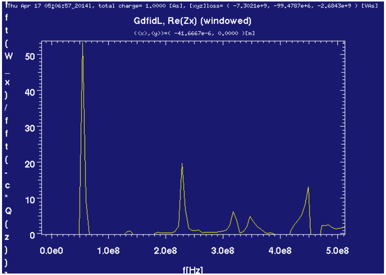

In order to investigate more in detail the low frequency HOMs, we performed a wire impedance measurement simulation for the collimator under study, benchmarking S-parameters results with real measurements recently carried out @ CERN

Details of the computation

Collimator Jaws half gap 3 mm, 0.25 mm wire radius, 1 mm mesh size, 4358 Million cells, Dipersive material blocks (ferrite), IBC on all metallic surfaces (Tungsten), 190 GB of RAM and 423000 timesteps for 30 days of computation on a 32 Cores, 4 Socket Opteron 6370P Server (Courtesy of W. Bruns)

S parameters results

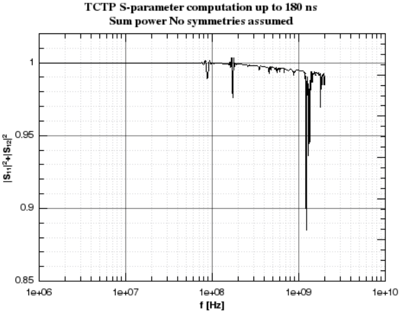

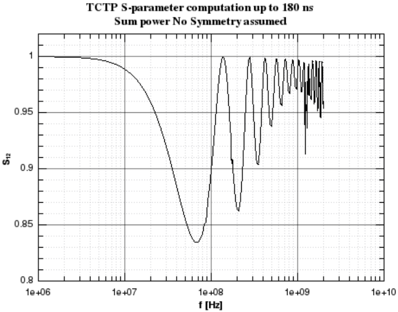

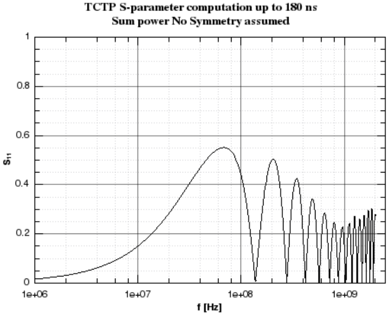

GdfidL computed modes

i	f [MHz]
1	87.0
2	173.0
3	1235.0

Simulated vs. measured modes

Complete measurements description, by N. Biancacci, available at
`https://indico.cern.ch/event/334750/`

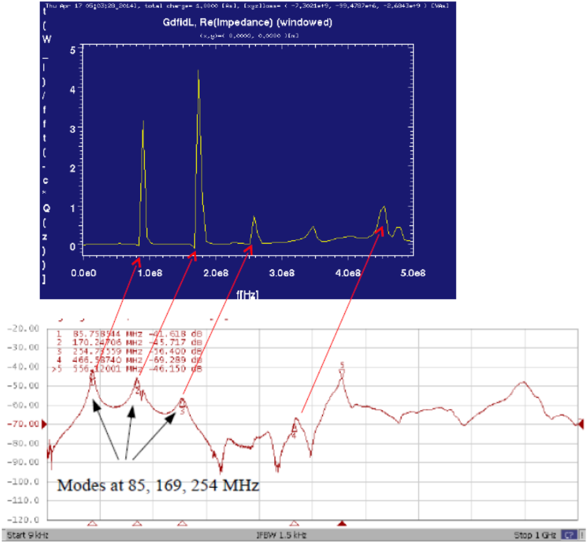

New TCS design concept

- One of the possible way to reduce the impedance of LHC secondary collimators is to reduce tapering angle;
- Present LHC secondary collimator design consists of two tapers at different angles, separated by a longitudinal gap, and at different distance from the beam axis; the closest to the beam contributes the most to the overall impedance;
- It has been shown that the best analytical approximation to the tapers' geometry is the Stupakov formula for flat taper [O. Frasciello et al., IPAC '14];
- Writing the impedance of the two tapers as a function of the first (the closest to the beam) taper angle and length, it is possible to find local minima and a best set of tapers' angles and lengths.

The analytical picture of the problem

Analytical total transverse impedance for two flat tapers separated by a longitudinal gap g, as a function of first taper's length L_1 and angle α_1:

$$
\begin{aligned}
Z_\perp &= \frac{Z_0 h_1}{8}\left(\frac{1}{a^2} - \frac{1}{\left(L_1 \tan\left(\alpha_1\right) + a\right)^2}\right)\tan\left(\alpha_1\right) \\
&+ \frac{\left(d - L_1 \tan\left(\alpha_1\right) - a\right) Z_0 h_2 \left(\frac{1}{\left(L_1 \tan(\alpha_1) + a\right)^2} - \frac{1}{d^2}\right)}{8\left(L - L_1 - g\right)}
\end{aligned}
$$

fixed parameters are the collimator half gap a, final height from the beam axis d, the gap g and total tapers' length $L = L_1 + L_2 + g$.

The geometrical sketch of the problem

$0^\circ \leq \alpha_1 \leq 45^\circ$; 18.7 mm $\leq L_1 \leq 97.4$ mm; $a = 1, 5, 20$ mm; $d - a = 18.7$ mm; $L = 147$ mm

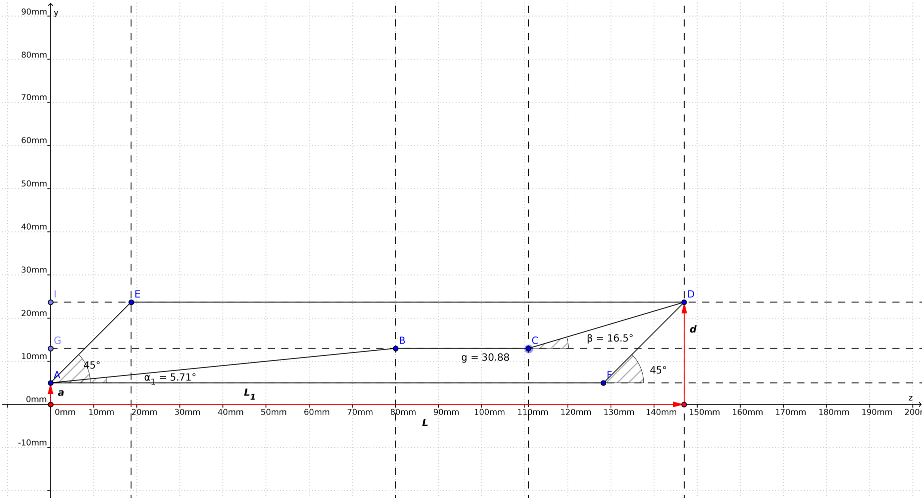

$Z_\perp$ as a function of a

L_1 [m], α_1 [rad], $Z_\perp$ [Ω/m] view

$a = 1$ mm

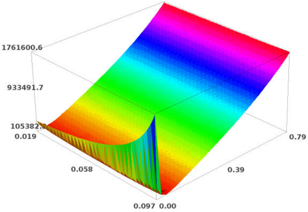

$a = 5$ mm

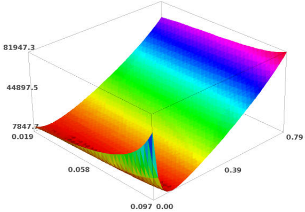

$a = 20$ mm

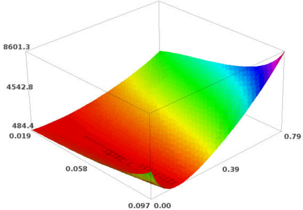

$Z_\perp$ for $a = 5$ mm

L_1 [m], $Z_\perp$ [Ω/m] plane view

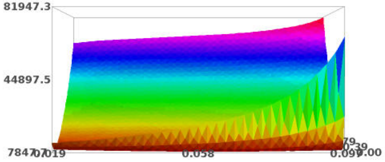

α_1 [rad], $Z_\perp$ [Ω/m] plane view

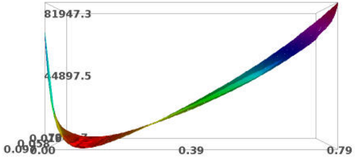

If all could be theoretically assessed...

Best set of lengths and angles for $Z_\perp$ local minimum

	$Z_{\perp_{min}}$ [kΩ/m]	L_1 [mm]	α_1 [°]	L_2 [mm]	α_2 [°]
$a = 1$mm	105.382	70	2.29	46.12	19.02
$a = 5$mm	7.848	64.4	4.7	51.7	14.5

Estimated gain wrt present LHC secondary collimator design ($\alpha_1 = 17.74°$, $L_1 = 25.78$ mm, $\alpha_2 = 16°$, $L_2 = 37.32$ mm)

	$Z_{\perp_{old}}/Z_{\perp_{min}}$
$a = 1$mm	5.2
$a = 5$mm	2.64

...but there are engineering contraints

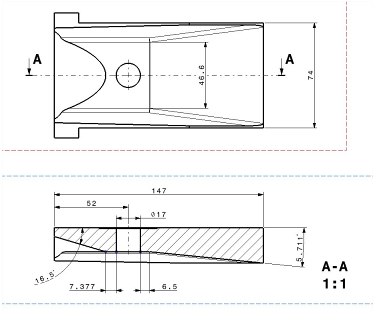

Old tapers angles : $Z_\perp$ (kΩ/m) = 26.24

New tapers angles : $Z_\perp$ (kΩ/m) = 11.74

Resistive wall contribution for the new angle set

The new (small) angles' set collimator design can, in principle, be affected by a stronger resistive wall (RW) contribution to the impedance, wrt the old one, expecially for small half gaps values. In order to estimate this contribution, again we carried out kick factors comparison for the two geometries, performing simulations for two flat tapers, using the new GdfidL version with implemented IBCs.

Simulated double flat taper geometry

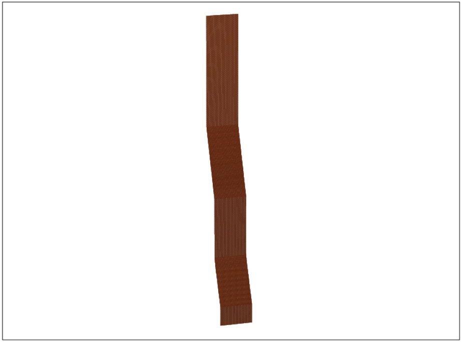

For old and new geometry the tapering angles are different

Resistive wall contribution for the new angle set

Material	σ [S/m], T = 20°C
PEC	∞
CFC	$1.4 \cdot 10^5$

RW data	Material
Old Collimator (BPM and large tapers' angles)	CFC
New Collimator (BPM and small tapers' angles)	CFC

half gap [mm]	$Z_\perp^{old}/Z_\perp^{new}$	$\lvert k_\perp^{old}\rvert/\lvert k_\perp^{new}\rvert$
1	≈ 3	≈ 1.3
5	≈ 2.6	≈ 2.1

$\sigma_b = 7.5$ cm, $s_{max} = 75$ cm wake computation for $k_\perp$ of LHC collimator designs

1 mm half gap	PEC	CFC
$k_\perp^{old}$ [V/Cm]	$9.31 \cdot 10^{14}$	$1.29 \cdot 10^{15}$
$k_\perp^{new}$ [V/Cm]	$7.20 \cdot 10^{14}$	$1.15 \cdot 10^{15}$

5 mm half gap	PEC	CFC
$k_\perp^{old}$ [V/Cm]	$4.47 \cdot 10^{13}$	$4.87 \cdot 10^{13}$
$k_\perp^{new}$ [V/Cm]	$2.17 \cdot 10^{13}$	$2.85 \cdot 10^{13}$

TDI designs: present one installed in LHC

Present TDI single segment geometry, one linear taper plus sharp discontinuity plus in & out 10 cm tubes, GdfidL wakefield simulations: $\sigma_z = 7.5$ cm, s=75 cm.

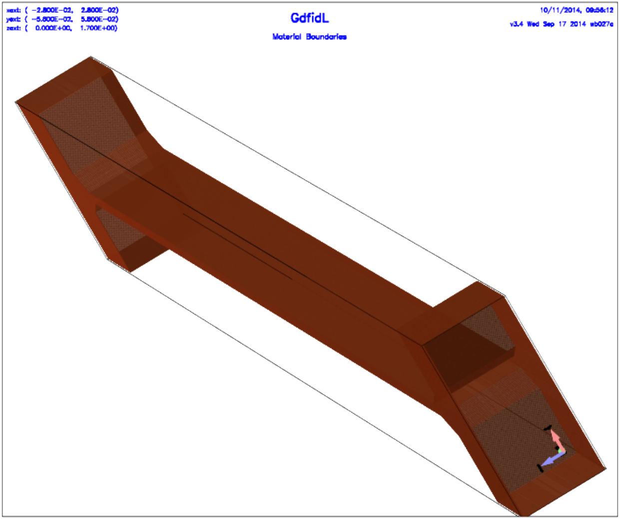

TDI designs: new one proposed by LHC collimation team

New proposed TDI single segment geometry, one linear taper plus in & out 10 cm tubes, GdfidL wakefield simulations: σ_z =7.5 cm, s=75 cm.

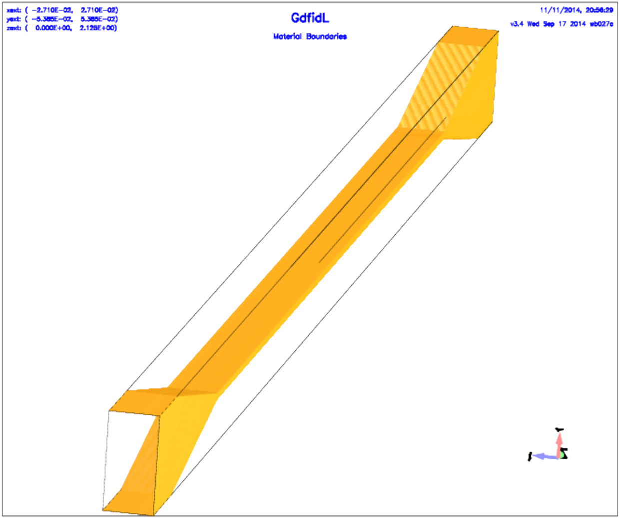

TDI designs: new one studied and suggested by INFN-LNF

New suggested TDI single segment geometry, plus in & out 10 cm tubes, GdfidL wakefield simulations: σ_z =7.5 cm, s=75 cm.

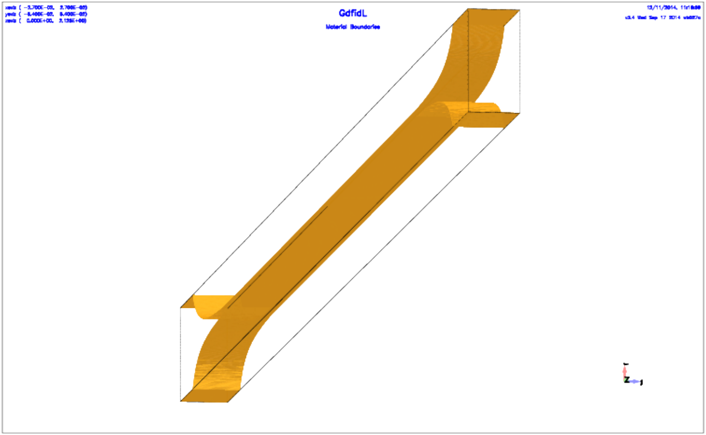

A non linear taper is described by a function of the type [2]: $h(z) = \frac{h_{min}}{[1+zL(\beta^{-\frac{1}{2}}-1)]^2}$,

where $\beta \equiv \frac{h_{max}}{h_{min}}$

[2] B.Podobedov and I.Zagorodnov, PAC2007, p. 2006

Resulting parameters from GdfidL simulations

PRESENT geometry (linear flat taper + sharp discontinuity)		
	PEC	R4550 graphite ($\sigma_\infty = 7.64 \cdot 10^4$ S/m)
$k_\parallel$ [V/C]	$1.73 \cdot 10^9$	$2.65 \cdot 10^9$
$Z_\perp(0)$ [kΩ/m]	49.4	123.1
$k_\perp$ [V/Cm]	$5.32 \cdot 10^{13}$	$1.37 \cdot 10^{14}$

NEW geometry (only longer and higher linear flat taper)		
	PEC	R4550 graphite ($\sigma_\infty = 7.64 \cdot 10^4$ S/m)
$k_\parallel$ [V/C]	$1.59 \cdot 10^9$	$2.75 \cdot 10^9$
$Z_\perp(0)$ [kΩ/m]	31.9	109.6
$k_\perp$ [V/Cm]	$3.46 \cdot 10^{13}$	$1.21 \cdot 10^{14}$

Alternative geometry (non linear taper)		
	PEC	R4550 graphite ($\sigma_\infty = 7.64 \cdot 10^4$ S/m)
$k_\parallel$ [V/C]	$1.61 \cdot 10^9$	$2.88 \cdot 10^9$
$Z_\perp(0)$ [kΩ/m]	19.98	102
$k_\perp$ [V/Cm]	$2.09 \cdot 10^{13}$	$1.11 \cdot 10^{14}$

Conclusions

For the present secondary collimator design

- The betatron tune shift was shown to be proportional to the transverse kick factor
- The collimator geometric impedance resulted to be not negligible with respect to the resisitive wall one
- LHC impedance model has been updated accordingly

For New TCTP design

- TT2-111R measured magnetic permeability was implemented into GdfidL code, by means of a 3rd order Lorentz function fit. S_{11} from coaxial cable measurement simulation was benchmarked with analytical formula and FD code HFSS, while ferrite filled pillbox longitudinal impedance with a MMM code and CST PS;
- In the new design new low frequency HOMs do appear, which are not damped by the used TT2-111R ferrite;
- On other hand, the ferrite is very effective in damping of the HOMs in the GHz region. A quite good agreement was found between low frequency HOMs detected by collimator wire measurements and wire measurements simulations with GdfidL, even though a full understanding of their nature (longitudinal or transverse) still deserves further investigations.

For TDI Collimators

- Resistive wall impedance computation by GdfidL was successfully tested;
- The TDI collimator jaws taper shape was optimized, including the geometric impedance and resistive walls.

The end...

Thanks for your kind attention

Appendix: Recent preliminary results on low freq HOMs damping

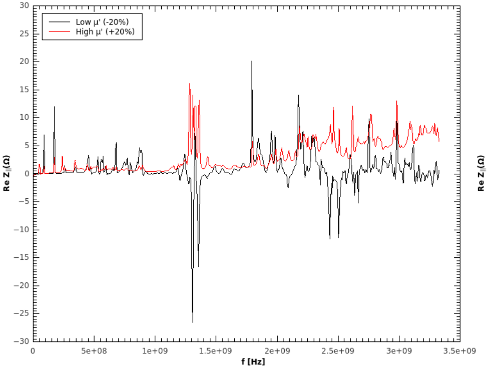

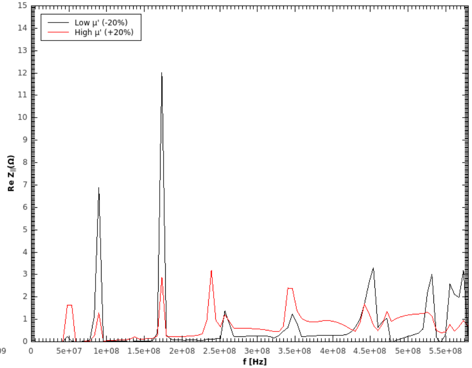

Appendix: How to test correct code μ implementation?

In our opinion it was a very useful method to arrange simple coaxial probe measurement simulations, in order to check for the numerically computed S-parameters to be fully in agreement with theoretical prediction.

Measurement layout (From R. Boni *et al.*, LNF-93/014)

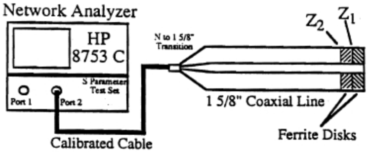

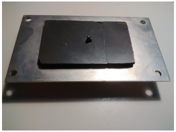

Simulated measurement

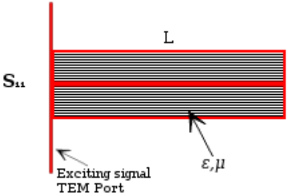

Analytical formulas

$$S_{11} = \frac{\Delta \cdot \tanh(\gamma L) - 1}{\Delta \cdot \tanh(\gamma L) + 1}; \qquad \gamma = j\omega\sqrt{\varepsilon\mu}; \qquad \Delta = \sqrt{\frac{\mu_r}{\varepsilon_r}}$$

Appendix: Theoretical considerations II exploited

Sacherer's formula for coherent mode frequency shift:

$$\boxed{\Delta\omega_{c_m} = j\frac{1}{1+|m|}\;\frac{I_c^2}{4\pi f_0 Q(E/e)L} Z_m^{eff}} \tag{4}$$

m azimuthal mode number; f_0 revolution frequency; I average bunch current; Q betatron tune; E machine energy; L full bunch length. The Z_m^{eff} is calculated over a coherent mode power spectrum:

$$Z_m^{eff} = \frac{\sum_p Z_T(\omega_p) h_m\left(\omega_p - \omega_\xi\right)}{\sum_p h_m \omega_p - \omega_\xi} \tag{5}$$

Appendix: Theoretical considerations II exploited

For a given mode m, the bunch power spectrum is given by:

$$h_m(\omega) = \left(\frac{\omega\sigma_z}{c}\right)^{2|m|} e^{-\left(\frac{\omega\sigma_z}{c}\right)^2} \tag{6}$$

The sum in 5 is performed over the mode spectrum lines:

$$\boxed{\omega_p = (p+\Delta Q)\omega_0 + m\omega_s \quad ; \quad -\infty < p < +\infty} \tag{7}$$

The "chromatic" angular frequency is given by

$$\omega_\xi = \omega_0 \frac{\xi}{\eta}$$

Appendix: Theoretical considerations II exploited

Given purely imaginary tune shifts from equation 4, they assume real values for imaginary transverse impedance. For $\xi = 0$ and coherent mode ($m = 0$) we get a proportionality relation:

$$\Delta\omega_{c_0} = -\mathrm{C}\cdot I\sum_{p}\Im Z_T\,(\omega_p)e^{-\left(\frac{\omega\sigma_z}{c}\right)^2} \tag{8}$$

But from kick factor definition:

$$k_T = \frac{1}{2\pi}\int_{-\infty}^{\infty}\Im Z_T(\omega)|\lambda(\omega)|^2\mathrm{d}\omega = \frac{1}{2\pi}\int_{-\infty}^{\infty}\Im Z_T(\omega)e^{-\left(\frac{\omega\sigma_z}{c}\right)^2}\mathrm{d}\omega \tag{9}$$

so that, comparing with 8, we find

$$\boxed{\Delta\omega_0 \propto -k_T} \tag{10}$$

Appendix: Theoretical considerations II exploited

In order to evaluate RW kicks, we can consider the thick wall impedance of a flat vacuum chamber with $2a \cdot 2b$ cross section:

$$\frac{Z_{T_y}}{L} = \frac{(1+j)Z_0\delta}{2\pi b^3} F_{1y}\left(\frac{b}{a}\right) \tag{11}$$

with $\delta = \sqrt{\frac{2c\rho}{\omega Z_0}}$ skin depth and $Z_0 = 120\ \pi\Omega$ free space impedance.

$$Z_{T_y} = \frac{L(1+j)Z_0\delta}{2\pi b^3} F_{1y}\left(\frac{b}{a}\right) = \frac{LZ_0\delta}{2\pi b^3} F_{1y}\left(\frac{b}{a}\right) + j\frac{LZ_0\delta}{2\pi b^3} F_{1y}\left(\frac{b}{a}\right)$$

$$\Im Z_T = \Im Z_{T_y} = \frac{LZ_0\delta}{2\pi b^3} F_{1y}\left(\frac{b}{a}\right) \tag{12}$$

Appendix: Theoretical considerations II exploited

Substituting 12 into 9 we get after some simple algebra:

$$k_T = \frac{L}{2\pi^2 b^3}\sqrt{2c\rho Z_0}F_{1y}\left(\frac{b}{a}\right)\int_0^\infty \frac{1}{\sqrt{\omega}}e^{-\frac{\omega^2\sigma_z^2}{c^2}}\mathrm{d}\omega;$$

$\int_0^\infty \frac{1}{\sqrt{\omega}}e^{-\frac{\omega^2\sigma_z^2}{c^2}}\mathrm{d}\omega$ is an Euler Γ function

$$\Gamma(z) = \int_0^\infty e^{-t}t^{z-1}\mathrm{d}t,$$

with $z = 0$. So that:

$$\int_0^\infty \frac{1}{\sqrt{\omega}}e^{-\frac{\omega^2\sigma_z^2}{c^2}}\mathrm{d}\omega = 2\Gamma\left(\frac{5}{4}\right)\frac{1}{\sqrt{\frac{\sigma_z}{c}}}$$

and we've

$$k_T = \frac{L}{2\pi^2 b^3}\sqrt{2c\rho Z_0}F_{1y}\left(\frac{b}{a}\right)2\sqrt{\frac{c}{\sigma_z}}\Gamma\left(\frac{5}{4}\right) \quad (13)$$

Appendix: Theoretical considerations II exploited

For a flat rectangular vacuum chamber, the form factor

$$F_{1y}\left(\frac{b}{a}\right) = \frac{\pi^2}{12}$$

so that, finally, the RW contributions:

$$\boxed{k_T = \frac{Lc}{12b^3}\sqrt{\frac{2Z_0\rho}{\sigma_z}}\Gamma\left(\frac{5}{4}\right)} \qquad (14)$$

Just as remark, note that the same type of calculations hold for $Z_T^x(\omega)$ but taking into account that $F_{1x}\left(\frac{b}{a}\right) = \frac{\pi^2}{24}$, so leading to a weaker vertical kick.

Comparison between LHC impedance model (RW) and equation 14

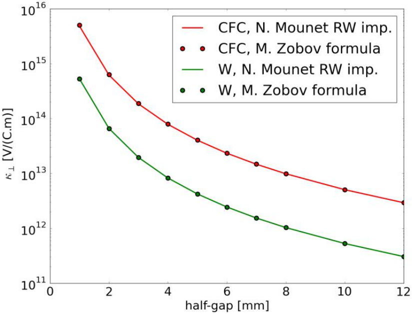

(Courtesy N. Mounet)